Organic & Biomolecular Chemistry

Cite this: *Org. Biomol. Chem.*, 2011, **9**, 3303

www.rsc.org/obc

PAPER

Conformational studies on peptides containing α,α-disubstituted α-amino acids: chiral cyclic α,α-disubstituted α-amino acid as an α-helical inducer†

Yosuke Demizu,*[a] Mitsunobu Doi,[b] Masaaki Kurihara,[a] Haruhiro Okuda,[a] Masanobu Nagano,[c] Hiroshi Suemune[c] and Masakazu Tanaka*[d]

Received 10th December 2010, Accepted 24th February 2011
DOI: 10.1039/c0ob01146k

Four types of α,α-disubstituted amino acids {*i.e.*, α-aminoisobutyric acid (Aib), 1-aminocyclopentanecarboxylic acid (Ac_5c), (3*S*,4*S*)-1-amino-(3,4-dimethoxy)cyclopentanecarboxylic acid [(*S*,*S*)-Ac_5c^{dOM}] and its enantiomer (*R*,*R*)-Ac_5c^{dOM}} were introduced into L-leucine-based hexapeptides and nonapeptides. The dominant conformations of eight peptides: Cbz-(L-Leu-L-Leu-dAA)$_2$-OMe [dAA = **1**: Aib; **2**: Ac_5c; **3**: (*S*,*S*)-Ac_5c^{dOM}; **4**: (*R*,*R*)-Ac_5c^{dOM}] and Boc-(L-Leu-L-Leu-dAA)$_3$-OMe [dAA = **5**: Aib; **6**: Ac_5c; **7**: (*S*,*S*)-Ac_5c^{dOM}; **8**: (*R*,*R*)-Ac_5c^{dOM}], were investigated by IR, CD spectra and X-ray crystallographic analysis. The CD spectra revealed that Aib hexapeptide **1** and Ac_5c hexapeptide **2** formed right-handed (*P*) 3_{10}-helices, while Ac_5c^{dOM} hexapeptides **3** and **4** formed a mixture of (*P*) 3_{10}- and α-helices. The Aib nonapeptide **5** formed a (*P*) 3_{10}-helix, the Ac_5c nonapeptide **6** formed a mixture of (*P*) 3_{10}- and α-helices, and the Ac_5c^{dOM} nonapeptides **7** and **8** formed (*P*) α-helices. X-Ray crystallographic analysis revealed that the Aib hexapeptide **1** formed a (*P*) 3_{10}-helix, while (*S*,*S*)-Ac_5c^{dOM} hexapeptide **3** formed a (*P*) α-helix. In addition, the Ac_5c nonapeptide **6** and (*R*,*R*)-Ac_5c^{dOM} nonapeptide **8** formed (*P*) α-helices. The Aib and achiral Ac_5c residues have the propensity to form 3_{10}-helices in short peptides, whereas the chiral Ac_5c^{dOM} residues have a penchant for forming α-helices.

Introduction

Precise control of the helical structures of peptides and proteins is highly important because they play a significant role in a variety of fields such as biological sciences, and material and medicinal chemistries.[1–4] To create such helical structures, utilization of α,α-disubstituted α-amino acids (dAAs) is a powerful method because the dAAs could restrict the conformational freedom of their peptides and stabilize the secondary structures.[5–12] Among them, α-aminoisobutyric acid (Aib), in which the α-hydrogen atom of L-alanine is replaced with a methyl substituent, has been widely used to stabilize helical structures of peptides.[13–19] We have recently reported that the introduction of Aib residues into the L-leucine-based hexapeptide (L-Leu-L-Leu-Aib-L-Leu-L-Leu-Aib) stabilized a right-handed (*P*) 3_{10}-helix, whereas that of 1-amino-(3,4-dimethoxy)cyclopentanecarboxylic acid (Ac_5c^{dOM}) residues,[20,21] which is a chiral cyclic dAA bearing only side-chain chiral centers,[22,23] stabilized a (*P*) α-helix in the solid state.[24,25] As a part of our ongoing research, we investigated the preferred conformations of four L-leucine-based hexapeptides, Cbz-(L-Leu-L-Leu-dAA)$_2$-OMe [dAA = **1**: Aib; **2**: Ac_5c; **3**: (*S*,*S*)-Ac_5c^{dOM}; **4**: (*R*,*R*)-Ac_5c^{dOM}] (Cbz: benzyloxycarbonyl, Ac_5c: 1-aminocyclopentanecarboxylic acid, OMe: methyl ester), and four nonapeptides, Boc-(L-Leu-L-Leu-dAA)$_3$-OMe [dAA = **5**: Aib; **6**: Ac_5c; **7**: (*S*,*S*)-Ac_5c^{dOM}; **8**: (*R*,*R*)-Ac_5c^{dOM}], in solution and in the crystalline state (Fig. 1). The IR and CD spectra, and X-ray crystallographic analysis revealed that the Aib and achiral Ac_5c residues have the tendency to form (*P*) 3_{10}-helices, whereas chiral cyclic dAA: (*S*,*S*)- and (*R*,*R*)-Ac_5c^{dOM}, have a penchant for forming (*P*) α-helices in short L-leucine-based peptides.

Results and discussion

Cyclic amino acids (*S*,*S*)-Ac_5c^{dOM} and (*R*,*R*)-Ac_5c^{dOM} were synthesized according to previously reported methods.[20,24] The preparation of hexapeptides **1–4** and nonapeptides **5–8** was carried out by a solution-phase method using 1-(3-dimethylaminopropyl)-3-ethylcarbodiimide (EDC) hydrochloride and 1-hydroxybenzotriazole (HOBt) hydrate as coupling reagents.[24–27]

[a]*Division of Organic Chemistry, National Institute of Health Sciences, Tokyo 158-8501, Japan. E-mail: demizu@nihs.go.jp; Fax: +81-3-3707-6950; Tel: +81-3-3700-1141*
[b]*Osaka University of Pharmaceutical Sciences, Osaka, 569-1094, Japan*
[c]*Graduate School of Pharmaceutical Sciences, Kyushu University, Fukuoka 812-8582, Japan*
[d]*Graduate School of Biomedical Sciences, Nagasaki University, Nagasaki 852-8521, Japan. E-mail: matanaka@nagasaki-u.ac.jp; Fax: +81-95-819-2423; Tel: +81-95-819-2423*

† Electronic supplementary information (ESI) available. CCDC reference numbers 602473–602475, 779688. For ESI and crystallographic data in CIF or other electronic format see DOI: 10.1039/c0ob01146k

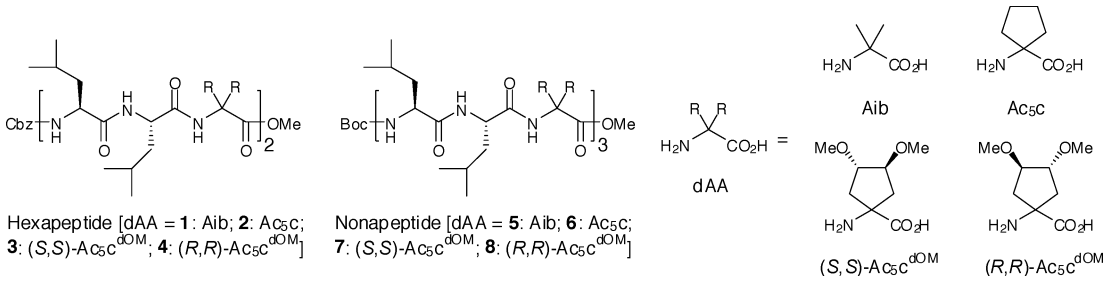

Hexapeptide [dAA = **1**: Aib; **2**: Ac_5c; **3**: (*S*,*S*)-Ac_5c^{dOM}; **4**: (*R*,*R*)-Ac_5c^{dOM}]

Nonapeptide [dAA = **5**: Aib; **6**: Ac_5c; **7**: (*S*,*S*)-Ac_5c^{dOM}; **8**: (*R*,*R*)-Ac_5c^{dOM}]

Fig. 1 Achiral and chiral α,α-disubstituted α-amino acids discussed in this paper.

Fig. 2 shows the FT-IR spectra of **1–8** in the NH-stretching region (amide A 3200–3500 cm^{-1}, peptide concentration 1.0 mM in $CDCl_3$ solution). The weak bands around the 3430 cm^{-1} region were assigned to free (solvated) peptide NH groups, and the strong bands around the 3320 cm^{-1} region were assigned to peptide NH groups with N—H···O═C intramolecular H-bonds. The IR spectra of hexa- and nonapeptides **1–8** were very similar to those of helical peptides in solution,[20,28] but different from those of peptides that form the extended planar C_5 conformation.[29,30] Furthermore, the Abs_{3320}/Abs_{3430} values of nonapeptides **5–8** increased compared with those of hexapeptides **1–4**, indicating that nonapeptides were more helical than hexapeptides.

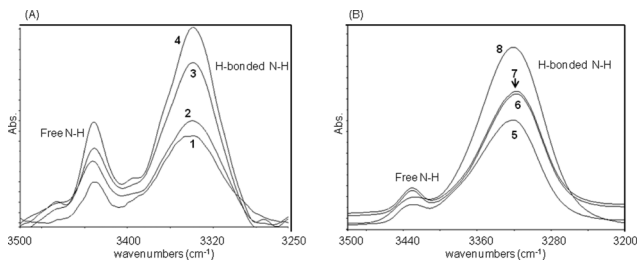

Fig. 2 FT-IR spectra (3200–3500 cm^{-1} region) of (A) hexapeptides Cbz-(L-Leu-L-Leu-dAA)$_2$-OMe [dAA = **1**: Aib; **2**: Ac_5c; **3**: (*S*,*S*)-Ac_5c^{dOM}; **4**: (*R*,*R*)-Ac_5c^{dOM}] and (B) nonapeptides Boc-(L-Leu-L-Leu-dAA)$_3$-OMe [dAA = **5**: Aib; **6**: Ac_5c; **7**: (*S*,*S*)-Ac_5c^{dOM}; **8**: (*R*,*R*)-Ac_5c^{dOM}] in $CDCl_3$ solution. Peptide concentration: 1.0 mM.

The CD spectra of peptides **1–8** were measured in a mixture of 2,2,2-trifluoroethanol (TFE) and H_2O (50/50) solution, and also in the solid state (KCl disk) to obtain information about their secondary structures. All CD spectra of **1–8** showed negative maxima at around 208 and 222 nm, indicating that the screw sense of the helices was right-handed (*P*) in solution and in the solid state (Fig. 3; red-shift of the maximum at 222 nm was observed in the solid state).[24,25] The ratio of *R* ($\theta_{222}/\theta_{208}$) in solution suggested that the dominant secondary structure of Aib hexapeptide **1** and Ac_5c hexapeptide **2** was a 3_{10}-helix (*R* = 0.5), and that of Ac_5c^{dOM} hexapeptides **3** and **4** (*R* = 0.6) was a mixture of 3_{10}- and α-helices (Fig. 3A).[24,31,32] In the solid state, the *R* values of **1** and **2** were 0.5 and those of **3** and **4** were 1.0 (Fig. 3B). These *R* values indicate that **1** with Aib and **2** with Ac_5c formed mainly (*P*) 3_{10}-helices, while **3** and **4** with Ac_5c^{dOM} formed α-helices. In the case of elongated nonapeptides, the preferred conformation of Aib nonapeptide **5** in solution was a 3_{10}-helix (*R* = 0.4), that of achiral Ac_5c nonapeptide **6** (*R* = 0.6) was a mixture of 3_{10}- and α-helices, and those of Ac_5c^{dOM} nonamers **7** and **8** (*R* = >0.7) were α-helices (Fig. 3C). In the solid

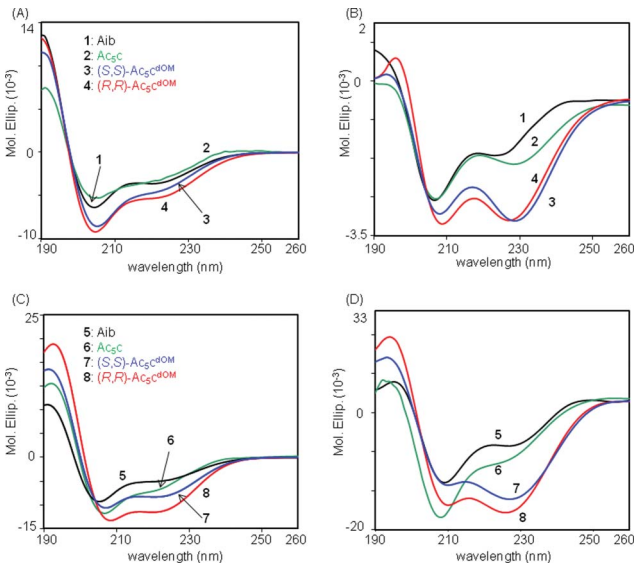

Fig. 3 CD spectra in the 190–260 nm region of peptides **1–8**. (A) Hexapeptides Cbz-(L-Leu-L-Leu-dAA)$_2$-OMe [dAA = **1**: Aib; **2**: Ac_5c; **3**: (*S*,*S*)-Ac_5c^{dOM}; **4**: (*R*,*R*)-Ac_5c^{dOM}] in TFE/H_2O = 50/50 solution, and (B) in KCl disk. (C) Nonapeptides Boc-(L-Leu-L-Leu-dAA)$_3$-OMe [dAA = **5**: Aib; **6**: Ac_5c; **7**: (*S*,*S*)-Ac_5c^{dOM}; **8**: (*R*,*R*)-Ac_5c^{dOM}] in TFE/H_2O = 50/50 solution, and (D) in KCl disk. Peptide concentration: 0.5 mM in TFE/H_2O solution; 0.5 mg peptides/70 mg KCl in the solid state.

state, a (*P*) 3_{10}-helix seemed to be present in **5** and **6** (*R* = 0.5), and α-helices seemed to be present in **7** and **8** (*R* = 1.1) (Fig. 3D).

The hexapeptides **1** and **3** and nonapeptides **6** and **8** became suitable crystals for X-ray crystallographic analysis by slow evaporation of the solvent (MeOH/H_2O for **1**, **3** and **8**, and EtOH/H_2O for **6**) at room temperature. The crystal and diffraction parameters of **1**, **3**, **6** and **8** are summarized in Table 1, and relevant backbone and side-chain torsion angles and the intra- and intermolecular hydrogen bond parameters are listed in Tables 2 and 3, respectively.

The crystal structure of Cbz-(L-Leu-L-Leu-Aib)$_2$-OMe (**1**) was a right-handed (*P*) 3_{10}-helix (Fig. 4) and solved in the space group *P*1. The mean values of the ϕ and ψ torsion angles of the amino acid residues (1–5) were −66.1° and −31.3°, respectively, which are close to those for an ideal right-handed (*P*) 3_{10}-helical structure (−60° and −30°).[33] Reversal of the torsion angle signs at the C-terminus occurred; that is, the signs of the ϕ and ψ torsion angles (+50.0° and +39.0°) of the Aib(6) residue were positive. Three consecutive intramolecular hydrogen bonds of the $i \leftarrow i+3$ type were present between H–N(4) and C(1)═O(1)

Table 1 Crystal and diffraction parameters of hexapeptides **1** and **3** and nonapeptides **6** and **8**

	1	**3**	**6**	**8**
Formula	$C_{41}H_{68}N_6O_9$	$2(C_{49}H_{80}N_6O_{13})$, CH_4O, H_2O	$4[C_{60}H_{105}N_9O_{12}$, $0.25(C_2H_6O)$, $1.5(H_2O)]$	$2(C_{66}H_{117}O_{18}N_9)$, CH_3OH, $5H_2O$
*M*r	789.01	1972.4	4732.31	2771.51
Crystal dimensions/mm	$0.50 \times 0.30 \times 0.20$	$0.60 \times 0.30 \times 0.10$	$0.30 \times 0.20 \times 0.05$	$0.30 \times 0.20 \times 0.05$
Crystal system	Triclinic	Triclinic	Monoclinic	Monoclinic
Lattice parameters:				
a/Å	10.411	12.903	15.449	11.561
b/Å	11.003	14.824	44.175	45.420
c/Å	11.330	16.669	21.677	15.286
α (°)	106.305	104.879	90	90
β (°)	94.754	93.483	96.234	95.52
γ (°)	103.828	112.918	90	90
V/Å^3	1193.8	2791.8	14706	7989.2
Space group	*P*1	*P*1	$P2_1$	$P2_1$
Z value	1	2	8	2
*D*calc/g cm^{-3}	1.097	1.173	1.069	1.152
μ(Mo-Kα)/cm^{-1}	0.77	0.86	0.75	0.85
No. of observations	3417 ($I > 2\sigma(I)$)	12192 ($I > 2\sigma(I)$)	21523 ($I > 2\sigma(I)$)	15919 ($I > 2\sigma(I)$)
No. of variables	2950	10971	3054	1739
R_1, *Rw*	0.0434, 0.0870	0.0522, 0.1427	0.0962, 0.2635	0.0859, 0.2370
Solvent	MeOH/H_2O	MeOH/H_2O	EtOH/H_2O	MeOH/H_2O

Table 2 Selected torsion angles ω, ϕ, ψ and χ (°) for hexapeptides **1** and **3** and nonapeptides **6** and **8** as determined by X-ray crystallographic analysis

		3		**6**				**8**	
Torsion angles	**1**	**A**	**B**	**A**	**B**	**C**	**D**	**A**	**B**
ω0	167.0	−170.7	−171.7	−170.9	−171.4	−166.9	−168.8	−170.6	173.5
ϕ1	−61.6	−50.1	−67.5	−74.9	−70.9	−71.2	−71.3	−70.6	−59.1
ψ1	−54.7	−51.3	− 26.3	−37.6	−39.6	−37.7	−36.1	−32.5	−18.4
ω1	−172.2	−167.3	178.4	176.6	−176.8	−177.8	−178.5	−179.4	170.3
ϕ2	−70.3	−67.6	−58.9	−72.5	−72.6	−73.3	−72.9	−71.1	−48.7
ψ2	−26.1	−34.8	−41.4	−43.3	−44.5	−42.9	−43.3	−47.2	−44.3
ω2	177.9	−180.0	−174.7	178.4	177.7	175.5	174.7	177.4	−174.7
ϕ3	−56.5	−60.7	−63.6	−55.1	−55.8	−54.3	−54.8	−54.6	−57.9
ψ3	−32.1	−44.0	−26.7	−45.8	−46.2	−47.0	−46.7	−49.0	−45.8
ω3	−176.9	−178.8	−178.9	−179.1	−177.9	−178.6	−176.1	179.6	179.6
ϕ4	−70.3	−72.6	−89.2	−69.0	−66.9	−65.6	−67.5	−57.5	−66.1
ψ4	−10.9	−34.3	−36.3	−46.1	−42.0	−46.5	−44.3	−48.3	−41.6
ω4	172.7	−177.1	−169.6	179.8	−179.7	−179.3	−178.0	−177.7	177.1
ϕ5	−71.6	−67.3	−99.6	−53.4	−55.1	−56.4	−62.5	−59.1	−58.0
ψ5	−32.6	−37.4	−11.4	−41.3	−40.7	−41.9	−34.2	−43.0	−42.6
ω5	−174.8	−174.7	−173.8	−177.9	−177.0	−176.1	176.5	−179.0	−179.2
ϕ6	50.0	56.6	64.9	−54.3	−54.7	−55.7	−53.8	−55.6	−56.2
ψ6	39.0	36.8	−167.7	−39.9	−39.4	−38.9	−41.7	−42.4	−44.1
ω6	173.7	177.1	−179.5	−179.6	−177.9	−176.4	−175.4	−175.7	178.4
ϕ7	—	—	—	−77.5	−83.2	−79.8	−82.4	−74.8	−66.9
ψ7	—	—	—	−40.3	−37.2	−39.0	−39.4	−34.1	−46.7
ω7	—	—	—	−172.5	−173.6	−176.6	−176.4	−176.6	−175.5
ϕ8	—	—	—	−78.3	−80.9	−79.7	−78.7	−87.1	−62.4
ψ8	—	—	—	−30.3	−35.9	−28.7	−36.3	−29.5	−34.9
ω8	—	—	—	−171.7	−176.3	−169.9	−173.5	−172.0	−179.3
ϕ9	—	—	—	60.0	49.2	61.6	49.1	55.4	51.3
ψ9	—	—	—	−153.8	39.4	−162.4	43.1	40.6	46.4
ω9	—	—	—	−172.7	−175.6	−175.9	−179.1	173.9	170.7
χ1	176.8	−179.5	−66.7	−62.4	−169.1	−65.2	−167.6	−55.5	−64.7
χ2	−79.7	−64.4	−176.6	−179.8	175.2	178.5	178.5	−179.0	175.4
χ3	—	107.7	72.6	115.0	100.3	142.7	120.1	100.5	86.9
χ3′	—	−135.2	−87.2	−129.0	−112.8	−152.7	−143.8	−128.3	−112.0
χ4	−62.2	−62.2	179.8	−169.8	−175.4	−176.7	−175.7	−70.7	−177.7
χ5	−174.1	−173.9	−57.7	−179.8	175.4	176.7	81.0	−176.0	179.5
χ6	—	98.4	94.2	74.4	72.4	74.6	75.3	83.0	83.5
χ6′	—	−121.3	−119.9	−81.5	−82.6	−81.5	−83.8	−76.6	−79.4
χ7	—	—	—	−59.0	−61.8	−61.9	−62.9	−70.6	−178.0
χ8	—	—	—	−59.0	−67.4	−63.1	−65.6	−72.5	−67.2
χ9	—	—	—	152.3	84.6	149.7	91.6	156.5	154.2
χ9′	—	—	—	−139.4	−81.0	−136.0	−109.5	−137.0	−132.9

Table 3 Intra- and intermolecular H-bond parameters for hexapeptides **1** and **3** and nonapeptides **6** and **8**

Peptide[a]	Donor	Acceptor	Distance/Å	Angle (°)	Symmetry operations
Cbz-(L-Leu-L-Leu-Aib)$_2$-OMe (**1**)[b]					
	N_3–H	O_0	3.42[c]	123.2	x,y,z
	N_4–H	O_1	3.20[d]	146.2	x,y,z
	N_5–H	O_2	2.99	159.5	x,y,z
	N_6–H	O_3	3.19[d]	149.4	x,y,z
	N_1–H	$O_{4'}$	2.92	164.1	x,y,−1+z
	N_2–H	$O_{5'}$	2.87	166.7	x,y,−1+z
Cbz-[L-Leu-L-Leu-(*S*,*S*)-Ac$_5$c^{dOM}]$_2$-OMe (**3**)					
Molecule **A**					
	N_{3a}–H	O_{0a}	3.24[d]	125.8	x,y,z
	N_{4a}–H	O_{0a}	3.49[c]	166.1	x,y,z
	N_{4a}–H	O_{1a}	3.27[d]	119.3	x,y,z
	N_{5a}–H	O_{1a}	2.99	150.4	x,y,z
	N_{6a}–H	O_{2a}	3.03	151.1	x,y,z
Molecule **B**[f]					
	N_{3b}–H	O_{0b}	3.20[d]	132.9	x,y,z
	N_{5b}–H	O_{1b}	2.92	145.2	x,y,z
	N_{6b}–H	O_{2b}	2.98	136.6	x,y,z
	N_{1b}–H	O_{5a}	2.91	151.1	x,y,z
	N_{2b}–H	O_{4a}	2.94	146.6	x,y,z
	O_{MeOH}–H[e]	O_{3b}	2.79	176.9	x,y,z
	O_w–H[e]	O_{MeOH}	2.80	173.7	x,y,z
	N_{2a}–H	$O_{w'}$	2.88	156.3	x,y,1+z
	O_w–H	$O_{5b'}$	2.72	173.6	1+x,y,z
Boc-(L-Leu-L-Leu-Ac$_5$c)$_3$-OMe (**6**)					
Molecule **A**					
	N_{4a}–H	O_{0a}	3.12	157.9	x,y,z
	N_{5a}–H	O_{1a}	2.89	159.3	x,y,z
	N_{6a}–H	O_{2a}	2.99	160.8	x,y,z
	N_{7a}–H	O_{4a}	2.98	128.2	x,y,z
	N_{8a}–H	O_{4a}	3.00	157.3	x,y,z
	N_{9a}–H	O_{5a}	2.85	152.5	x,y,z
	N_{2a}–H	O_{wa}	3.00	124.1	x,y,z
	N_{3a}–H	O_{wa}	3.00	167.9	x,y,z
	N_{1a}–H	$O_{8a'}$	2.87	162.0	−1+x,y,z
	O_{wa}–H	$O_{7a'}$	2.89	176.6	−1+x,y,z
Molecule **B**					
	N_{3b}–H	O_{0b}	3.20[d]	132.9	x,y,z
	N_{4b}–H	O_{0b}	3.08	158.3	x,y,z
	N_{5b}–H	O_{1b}	2.86	155.6	x,y,z
	N_{6b}–H	O_{2b}	3.09	154.7	x,y,z
	N_{7b}–H	O_{4b}	3.02	131.7	x,y,z
	N_{8b}–H	O_{4b}	2.96	154.6	x,y,z
	N_{9b}–H	O_{5b}	2.94	168.9	x,y,z
	O_{wb}–H	O_{6b}	2.91	173.0	x,y,z
	O_{wb}–H	O_{wc}	2.77	172.6	x,y,z
	O_{wc}–H	O_{7b}	2.83	171.3	x,y,z
	N_{1b}–H	$O_{8b'}$	2.85	167.0	−1+x,y,z
	N_{2b}–H	$O_{wc'}$	3.05	125.5	−1+x,y,z
	N_{3b}–H	$O_{wc'}$	3.05	169.9	−1+x,y,z
Molecule **C**					
	N_{4c}–H	O_{0c}	3.15	159.7	x,y,z
	N_{5c}–H	O_{1c}	2.84	158.2	x,y,z
	N_{6c}–H	O_{2c}	2.96	160.2	x,y,z
	N_{7c}–H	O_{4c}	3.06	150.1	x,y,z
	N_{8c}–H	O_{4c}	3.00	157.1	x,y,z
	N_{9c}–H	O_{5c}	2.87	147.4	x,y,z
	O_{wd}–H	O_{7c}	2.90	170.8	x,y,z
	N_{1c}–H	$O_{8c'}$	2.85	159.3	1+x,y,z
	N_{2c}–H	$O_{wd'}$	2.99	128.7	1+x,y,z
	N_{3c}–H	$O_{wd'}$	3.13[d]	167.1	1+x,y,z
Molecule **D**					
	N_{4d}–H	O_{0d}	3.06	155.8	x,y,z
	N_{5d}–H	O_{1d}	2.86	157.4	x,y,z
	N_{6d}–H	O_{2d}	3.10	161.3	x,y,z
	N_{7d}–H	O_{4d}	3.04	130.8	x,y,z

Table 3 *(Contd.)*

Peptide[a]	Donor	Acceptor	Distance/Å	Angle (°)	Symmetry operations
	N_{8d}–H	O_{4d}	2.93	157.4	x,y,z
	N_{9d}–H	O_{5d}	2.95	162.8	x,y,z
	N_{2d}–H	O_{we}	3.01	129.6	x,y,z
	N_{3d}–H	O_{we}	3.17[d]	168.3	x,y,z
	O_{wf}–H	O_{we}	2.72	170.8	x,y,z
	N_{1d}–H	$O_{8d'}$	2.81	166.5	1+x,y,z
	O_{we}–H	$O_{7d'}$	2.89	177.2	1+x,y,z
	O_{wf}–H	$O_{6d'}$	2.89	175.5	1+x,y,z
Boc-[L-Leu-L-Leu-(*R*,*R*)-Ac_5c^{dOM}]$_3$-OMe (**8**)					
Molecule **A**					
	N_{4a}–H	O_{0a}	3.16	166.0	x,y,z
	N_{5a}–H	O_{1a}	2.87	156.5	x,y,z
	N_{6a}–H	O_{2a}	2.93	166.6	x,y,z
	N_{7a}–H	O_{3a}	3.27[d]	156.2	x,y,z
	N_{8a}–H	O_{4a}	2.94	147.4	x,y,z
	N_{9a}–H	O_{5a}	2.82	149.7	x,y,z
	O_{wa}–H	O_{6a}	2.87	173.7	x,y,z
	O_{wb}–H	O_{9a}	2.79	174.0	x,y,z
	O_{wa}–H	O_{wc}	2.82	179.1	x,y,z
	N_{1a}–H	$O_{8a'}$	2.83	149.1	x,y,1+z
	N_{2a}–H	$O_{wc'}$	2.94	129.4	x,y,1+z
	N_{3a}–H	$O_{wc'}$	3.20[d]	164.4	x,y,1+z
	O_{wb}–H	$O_{wa'}$	3.02	169.8	1+x,y,z
Molecule **B**					
	N_{3b}–H	O_{0b}	3.01	149.2	x,y,z
	N_{5b}–H	O_{1b}	2.89	166.0	x,y,z
	N_{6b}–H	O_{2b}	2.92	160.3	x,y,z
	N_{7b}–H	O_{3b}	3.40[c]	159.4	x,y,z
	N_{8b}–H	O_{4b}	2.85	162.2	x,y,z
	N_{9b}–H	O_{5b}	2.91	157.7	x,y,z
	O_{wd}–H	O_{6b}	3.06	172.1	x,y,z
	O_{we}–H	O_{wd}	2.64	175.6	x,y,z
	O_{we}–H	O_{MeOH}	2.87	175.4	x,y,z
	O_{MeOH}–H	O_{M9}[e]	2.77	173.6	x,y,z
	N_{1b}–H	$O_{7b'}$	2.82	164.4	x,y,1+z
	N_{2b}–H	$O_{wd'}$	2.89	162.7	x,y,1+z

[a] The amino acid numbering begins at the N-terminus of the peptide chain. [b] The hydrogen bond between N_4–H and O_0 (3.71 Å) in hexapeptide **1** is not observed. [c] The D···A distance is too long for a hydrogen bond. [d] The D···A distance is a bit long for a hydrogen bond. [e] O_w: water; O_{MeOH}: MeOH; O_M: methoxy group. [f] The hydrogen bond between N_{4b}–H and O_{0b} (3.76 Å) in hexapeptide **3** is not observed.

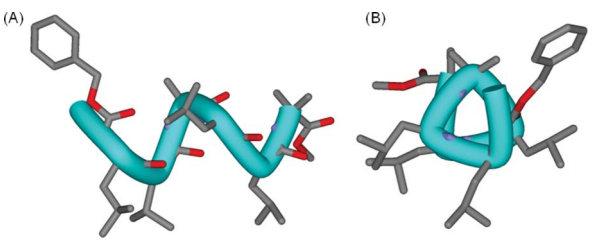

Fig. 4 X-Ray diffraction structure of Cbz-(L-Leu-L-Leu-Aib)$_2$-OMe (**1**) as viewed (A) perpendicular to and (B) along the helical axis.

[N(4)···O(1) = 3.20 Å; N–H···O 146.2°], H–N(5) and C(2)═O(2) [N(5)···O(2) = 2.99 Å; N–H···O 159.5°], and H–N(6) and C(3)═O(3) [N(6)···O(3) = 3.19 Å; N–H···O 149.4°], although the distances between H–N(3) and C(0)═O(0) [N(3)···O(0) = 3.42 Å; N–H···O 123.2°] (β-turn) and H–N(4) and C(0)═O(0) [N(4)···O(0) = 3.71 Å; N–H···O 140.8°] (α-turn) were too long for hydrogen bonds.

In the packing mode, two intermolecular hydrogen bonds were observed between the 3_{10}-helical conformers; that is, between the H–N(1) donor and the C(4′)═O(4′) O atom of a symmetry-related molecule (x, y, −1+z) [N(1)···O(4′) = 2.92 Å; N–H···O 164.1°] and between the H–N(2) donor and the C(5′)═O(5′) O atom of a symmetry-related molecule (x, y, −1+z) [N(2)···O(5′) = 2.87 Å; N–H···O 166.7°]. The helical molecules were connected by intermolecular hydrogen bonds forming a head-to-tail alignment of chains (Fig. 5).

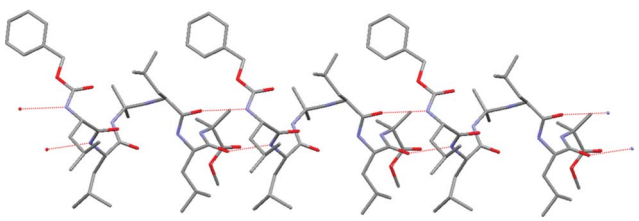

Fig. 5 Packing of **1** in the crystalline state. Intermolecular hydrogen bonds are indicated as red dashed lines.

Cbz-[L-Leu-L-Leu-(*S*,*S*)-Ac_5c^{dOM}]$_2$-OMe (**3**) exclusively crystallized into two right-handed (*P*) α-helical conformers **A** and **B** with a methanol and a water molecule (Fig. 6). The peptide-main chain conformations of molecules **A** and **B** were similar except

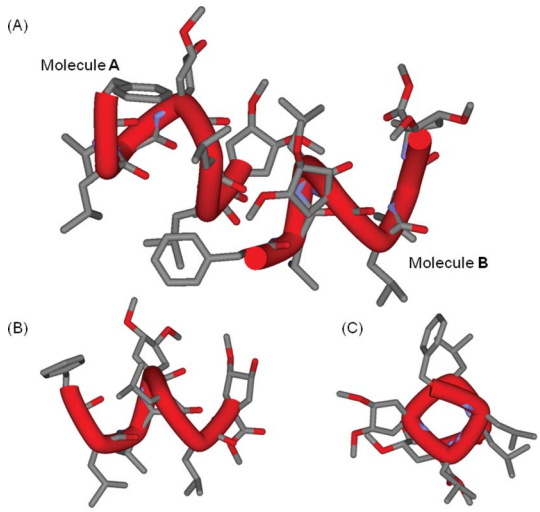

Fig. 6 (A) X-Ray diffraction structure of Cbz-[L-Leu-L-Leu-(*S*,*S*)-Ac_5c^{dOM}]$_2$-OMe (**3**). The methanol and water molecules are omitted. The structure of molecule **A**, as viewed (B) perpendicular to and (C) along the helical axis.

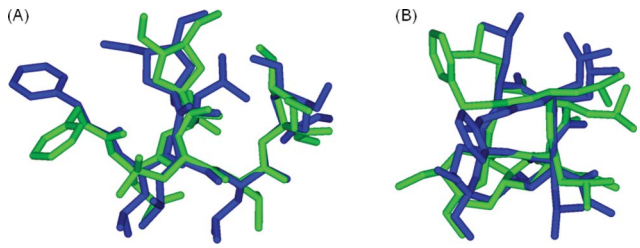

Fig. 7 The overlaid structures of molecules **A** (green) and **B** (blue), as viewed (A) perpendicular to and (B) along the helical axis.

for differences in the conformations of the N-terminal protecting group and their side chains, especially at L-Leu(5) and Ac_5c^{dOM}(6) residues, as shown by their superimposition in Fig. 7. The mean values of the ϕ and ψ torsion angles of the amino acid residues (1–5) were –63.7° and –40.4° for molecule **A** and –75.8° and –28.4° for molecule **B**, and reversal of the torsion angle signs at the C-terminus occurred. The average torsion angles of molecule **A** were close to those for an ideal right-handed (*P*) α-helical structure (–60° and –45°), while those of molecule **B** seemed to be a distorted (*P*) α-helix with semi-extended conformation at L-Leu(5B) (ϕ = –99.6°, ψ = –11.4°) and Ac_5c^{dOM}(6B) (ϕ = +64.9°, ψ = –167.7°). In molecule **A**, two intramolecular hydrogen bonds of the $i \leftarrow i$+4 type were observed between H–N(5a) and C(1a)═O(1a) [N(5a)···O(1a) = 2.99 Å; N–H···O 150.4°] and H–N(6a) and C(2a) = O(2a) [N(6a)···O(2a) = 3.03 Å; N–H···O 151.1°]. Furthermore, two weak intramolecular hydrogen bonds of the $i \leftarrow i$+3 (β-turn) type were observed between H–N(3a) and C(0a)═O(0a) [N(3a)···O(0a) = 3.24 Å; N–H···O 125.8°] and between H–N(4a) and C(1a)═O(1a) [N(4a)···O(1a) = 3.27 Å; N–H···O 119.3°], but the distance between H–N(4a) and C(0a)═O(0a) [N(4a)···O(0a) = 3.49 Å; N–H···O 166.1°] was too long for a hydrogen bond of the $i \leftarrow i$+4 (α-turn) type. Molecule **B** similarly contained two intramolecular hydrogen bonds between H–N(5b) and C(1b)═O(1b) [N(5b)···O(1b) = 2.92 Å; N–H···O 145.2°] and H–N(6b) and C(2b)═O(2b) [N(6b)···O(2b) = 2.98 Å; N–H···O 136.6°], and the distance between H–N(4b) and C(0b)═O(0b) for α-turn [N(4b)···O(0b) = 3.76 Å; N–H···O 140.1°] was too long for a hydrogen bond. Furthermore, one weak intramolecular hydrogen bond of the $i \leftarrow i$+3 (β-turn) type was observed between H–N(3b) and C(0b)═O(0b) [N(3b)···O(0b) = 3.20 Å; N–H···O 132.9°]. In the packing mode, six intermolecular hydrogen bonds were observed between the H–N(1b) donor and the C(5a)═O(5a) acceptor [N(1b)···O(5a) = 2.91 Å; N–H···O 151.1°], H–N(2b) and C(4a)═O(4a) [N(2b)···O(4a) = 2.94 Å; N–H···O 146.6°], the H–O_{MeOH} of the methanol donor and C(3b)═O(3b) [O_{MeOH}···O(3b) = 2.79 Å; O–H···O 176.9°], the H–O_w of the water donor and O_{MeOH} of the methanol acceptor [O_W···O_{MeOH} = 2.80 Å; O–H···O 173.7°], the H–N(2a) and $O_{w'}$ [N(2a)···$O_{w'}$ = 2.88 Å; N–H···O 156.3°] of a symmetry-related molecule (x, y, 1+z), and the H–O_w and C(5b′)═O(5b′) [O_w···O(5b′) = 2.72 Å; N–H···O 173.6°] of a symmetry-related molecule (1+x, y, z). Molecules **A** and **B** were alternately connected, as shown in Fig. 8.

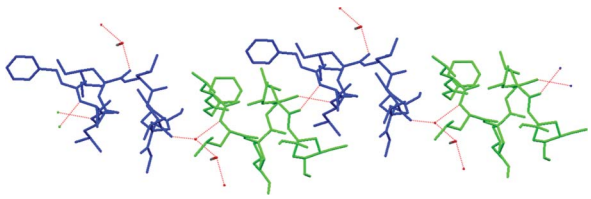

Fig. 8 Packing of **3** (molecule **A**: green, molecule **B**: blue) in the crystalline state. Intermolecular hydrogen bonds are indicated as red dashed lines.

The structure of Boc-(L-Leu-L-Leu-Ac_5c)$_3$-OMe (**6**) was solved in the space group $P2_1$.[34] Four crystallographically independent molecules **A**, **B**, **C** and **D** were found in the asymmetric unit together with an ethanol and water molecules. All molecules **A–D** were folded into α-helical structures (Fig. 9), and the main-chain conformations of peptides **A–D** were well matched except for small differences in the conformations of their side chains (Fig. 10). The mean values of the ϕ and ψ torsion angles of the amino acid residues (1–8) were –66.9° and –40.6° for **A**, –67.5° and –40.7° for **B**, –67.0° and –40.3° for **C**, –68.0° and –40.3° for **D**. Flip of the torsion angles at the C-terminus residue occurred, that is, the values of the ϕ and ψ torsion angles of the Ac_5c(9) were +60.0°, –153.8° for **A**; +49.2°, +39.4° for **B**; +61.6°, –162.4° for **C**; and +43.1°, –179.1° for **D**. In molecules **A–D**, five hydrogen bonds of the $i \leftarrow i$+4 type were observed between H–N(4a–d) and C(0a–d)═O(0a–d) [N(4a–d)···O(0a–d) = 3.12 Å (a), 3.08 Å (b), 3.15 Å (c), 3.06 Å (d); N–H···O 157.9° (a), 158.3° (b), 159.7° (c), 155.8°

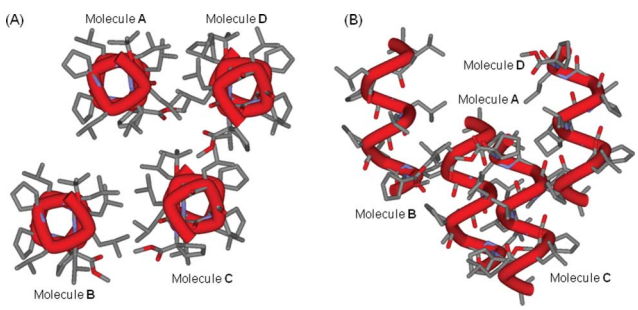

Fig. 9 X-Ray diffraction structure of Boc-(L-Leu-L-Leu-Ac_5c)$_3$-OMe (**6**), as viewed (A) perpendicular to and (B) along the helical axis. The ethanol and water molecules have been omitted.

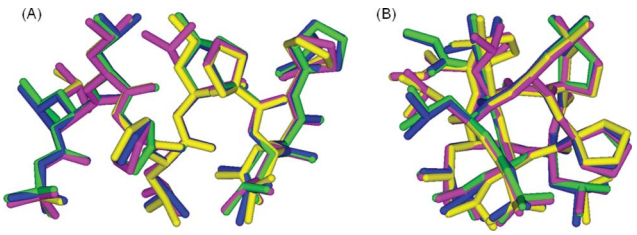

Fig. 10 The overlaid structures of molecules **A** (blue), **B** (purple), **C** (green) and **D** (yellow), as viewed (A) perpendicular to and (B) along the helical axis.

(d)], H–N(5a–d) and C(1a–d)═O(1a–d) [N(5a–d)···O(1a–d) = 2.89 Å (a), 2.86 Å (b), 2.84 Å (c), 2.86 Å (d); N–H···O 159.3° (a), 155.6° (b), 158.2° (c), 157.4° (d)], H–N(6a–d) and C(2a–d)═O(2a–d) [N(6a–d)···O(2a–d) = 2.99 Å (a), 3.09 Å (b), 2.96 Å (c), 3.10 Å (d); N–H···O 160.8° (a), 154.7° (b), 160.2° (c), 161.3° (d)], H–N(8a–d) and C(4a–d)═O(4a–d) [N(8a–d)···O(4a–d) = 3.00 Å (a), 2.96 Å (b), 3.00 Å (c), 2.93 Å (d); N–H···O 157.3° (a), 154.6° (b), 157.1° (c), 157.4° (d)], and H–N(9a–d) and C(5a–d)═O(5a–d) [N(9a–d)···O(5a–d) = 2.85 Å (a), 2.94 Å (b), 2.87 Å (c), 2.95 Å (d); N–H···O 152.5° (a), 168.9° (b), 147.4° (c), 162.8° (d)]. Furthermore, one hydrogen bond of $i \leftarrow i+3$ type between H–N(7a–d) and C(4a–d)═O(4a–d) [N(7a–d)···O(4a–d) = 2.98 Å (a), 3.02 Å (b), 3.06 Å (c), 3.04 Å (d); N–H···O 128.2° (a), 131.7° (b), 150.1° (c), 130.8° (d)] was observed. In the packing mode of molecule **A**, four intermolecular hydrogen bonds were observed between the H–N(2a) donor and O_w(a) of the water (a) acceptor [N(2a)···O_w(a) = 3.00 Å; N–H···O 124.1°], H–N(3a) and O_w(a) [N(3a)···O_w(a) = 3.00 Å; N–H···O 167.9°], the H–N(1a) and C(8a′)═O(8a′) [N(1a)···O(8a′) = 2.87 Å; N–H···O 162.0°] of a symmetry-related molecule (–1+x, y, z), and the H–O_w(a) and C(7a′)═O(7a′) [O_w(a)···O(7a′) = 2.89 Å; O–H···O 176.6°] of a symmetry-related molecule (–1+x, y, z). For molecule **B**, six intermolecular hydrogen bonds were observed between H–O_w(b) and C(6b)═O(6b) [O_w(b)···O(6b) = 2.91 Å; O–H···O 173.0°], H–O_w(b) and O_w(c) [O_w(b)···O_w(c) = 2.77 Å; O–H···O 172.6°], H–O_w(c) and C(7b)═O(7b) [O_w(c)···O(7b) = 2.83 Å; O–H···O 171.3°], the H–N(1b) and C(8b′)═O(8b′) [N(1b)···O(8b′) = 2.85 Å; N–H···O 167.0°] of a symmetry-related molecule (–1+x, y, z), the H–N(2b) and O_w(c′) [N(2b)···O_w(c′) = 3.05 Å; N–H···O 125.5°] of a symmetry-related molecule (–1+x, y, z), and the H–N(3b) and O_w(c′) [N(3b)···O_w(c′) = 3.05 Å; N–H···O 169.9°] of a symmetry-related molecule (–1+x, y, z). For molecule **C**, four intermolecular hydrogen bonds were observed between H–O_w(d) and C(7c)═O(7c) [O_w(d)···O(7c) = 2.90 Å; O–H···O 170.8°], the H–N(1c) and C(8c′)═O(8c′) [N(1c)···O(8c′) = 2.85 Å; N–H···O 159.3°] of a symmetry-related molecule (1+x, y, z), the H–N(2c) and O_w(d′) [N(2c)···O_w(d′) = 2.99 Å; N–H···O 128.7°] of a symmetry-related molecule (1+x, y, z), and the H–N(3c) and O_w(d′) [N(3c)···O_w(d′) = 3.13 Å (a bit long for an intermolecular hydrogen bond); N–H···O 167.1°] of a symmetry-related molecule (1+x, y, z). For molecule **D**, six intermolecular hydrogen bonds were observed between H–N(2d) and O_w(e) [N(2d)···O_w(e) = 3.01 Å; N–H···O 129.6°], H–N(3d) and O_w(e) [N(3d)···O_w(e) = 3.17 Å (a bit long for an intermolecular hydrogen bond); N–H···O 168.3°], H–O_w(f) and O_w(e) [O_w(f)···O_w(e) = 2.72 Å; O–H···O 170.8°], the H–N(1d) and C(8d′)═O(8d′) [N(1d)···O(8d′) = 2.81 Å; N–H···O 166.5°] of a symmetry-related molecule (1+x, y, z), the H–O_w(e) and C(7d′)═O(7d′) [O_w(e)···O(7d′) = 2.89 Å; O–H···O 177.2°] of a symmetry-related molecule (1+x, y, z), and the H–O_w(f) and C(6d′)═O(6d′) [O_w(f)···O(6d′) = 2.89 Å; O–H···O 175.5°] of a symmetry-related molecule (1+x, y, z). The four helical molecules **A–D** were connected by water molecule-mediated intermolecular hydrogen bonds, forming a head-to-tail alignment of chains ···**A**···**A**···**A**···, ···**B**···**B**···**B**···**B**···, ···**C**···**C**···**C**···**C**··· and ···**D**···**D**···**D**···**D**···, respectively (Fig. 11).

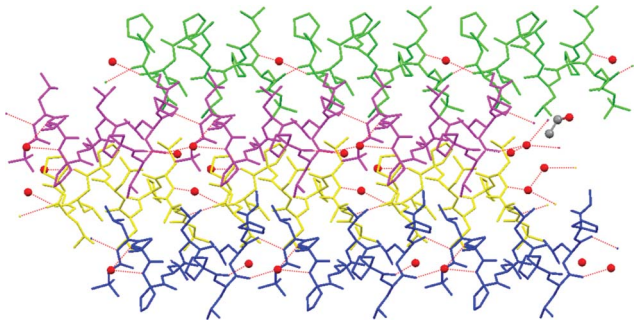

Fig. 11 Packing of **6** (molecule **A**: blue, molecule **B**: purple, molecule **C**: green, molecule **D**: yellow) in the crystalline state. Intermolecular hydrogen bonds are indicated as red dashed lines.

In the asymmetric unit of Boc-[L-Leu-L-Leu-(*R*,*R*)-Ac_5c^{dOM}]$_3$-OMe (**8**), two right-handed (*P*) α-helices were present with methanol and water molecules (Fig. 12). The conformations of the two molecules **A** and **B** were generally similar (Fig. 13), except for small differences at the N-terminus and at the side chains of the Leu and Ac_5c^{dOM} residues, and for the pattern of intramolecular hydrogen bonds. The mean values of the ϕ and ψ torsion angles of the amino acid residues (1–8) were –66.3° and –40.8° for **A**, –59.4° and –39.8° for **B**, and reversal of the torsion angle signs at the C-terminus occurred at the Ac_5c^{dOM}(9) residue (ϕ,ψ = +55.4°, +40.6° for **A** and

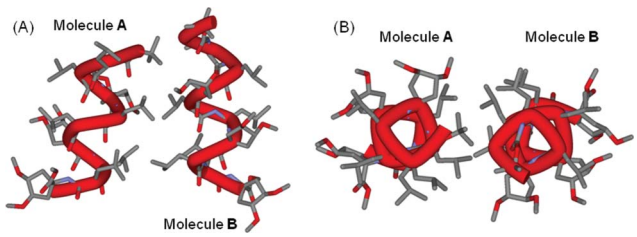

Fig. 12 X-Ray diffraction structure of Boc-[L-Leu-L-Leu-(*R*,*R*)-Ac_5c^{dOM}]$_3$-OMe (**8**), as viewed (A) perpendicular to and (B) along the helical axis. The methanol and water molecules are omitted.

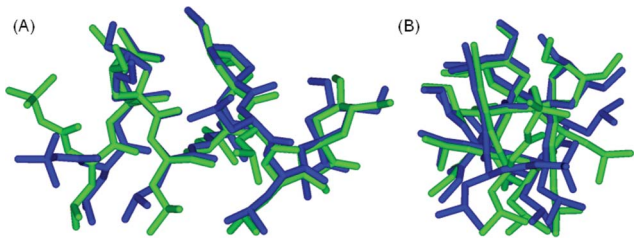

Fig. 13 The overlaid structures of molecules **A** (blue) and **B** (green), as viewed (A) perpendicular to and (B) along the helical axis.

ϕ,ψ = +51.3°, +46.4° for **B**). In molecule **A**, five intramolecular hydrogen bonds of the $i \leftarrow i$+4 type between H–N(4a) and C(0a)═O(0a) [N(4a)···O(0a) = 3.16 Å; N–H···O 166.0°], H–N(5a) and C(1a)═O(1a) [N(5a)···O(1a) = 2.87 Å; N–H···O 156.5°], H–N(6a) and C(2a) = O(2a) [N(6a)···O(2a) = 2.93 Å; N–H···O 166.6°], H–N(8a) and C(4a)═O(4a) [N(8a)···O(4a) = 2.94 Å; N–H···O 147.4°], and H–N(9a) and C(5a)═O(5a) [N(9a)···O(5a) = 2.82 Å; N–H···O 149.7°] were observed. Furthermore, one weak intramolecular hydrogen bond was observed between H–N(7a) and C(3a)═O(3a) [N(7a)···O(3a) = 3.27 Å; N–H···O 156.2°]. In the packing mode, six intermolecular hydrogen bonds between H–O_w(a) and C(6a)═O(6a) [O_w(a)···O(6a) = 2.87 Å; O–H···O 173.7°], H–O_w(b) and C(9a)═O(9a) [O_w(b)···O(9a) = 2.79 Å; O–H···O 174.0°], H–O_w(a) and O_w(c) [O_w(a)···O_w(c) = 2.82 Å; O–H···O 179.1°], H–N(1a) and C(8a′)═O(8a′) [N(1a)···O(8a′) = 2.83 Å; N–H···O 149.1°] of a symmetry-related molecule (x, y, 1+z), the H–N(2a) and O_w(c′) [N(2a)···O_w(c′) = 2.94 Å; N–H···O 129.4°] of a symmetry-related molecule (x, y, 1+z), the H–O_w(b) and O_w(a′) [O_w(b)···O_w(a′) = 3.02 Å; O–H···O 169.8°] of a symmetry-related molecule (1+x, y, z), and one weak intermolecular hydrogen bond between the H–N(3a) and O_w(c′) [N(3a)···O_w(c′) = 3.20 Å; N–H···O 169.8°] of a symmetry-related molecule (x, y, 1+z) were observed. In contrast to the $i \leftarrow i$+4-type hydrogen bonds of molecule **A**, in molecule **B**, one intramolecular hydrogen bond of the $i \leftarrow i$+3 type between H–N(3b) and C(0b)═O(0b) [N(3b)···O(0a) = 3.01 Å; N–H···O 149.2°] was observed. In addition, four intramolecular hydrogen bonds of the $i \leftarrow i$+4 type between H–N(5b) and C(1b)═O(1b) [N(5b)···O(1b) = 2.89 Å; N–H···O 166.0°], H–N(6b) and C(2b)═O(2b) [N(6b)···O(2b) = 2.92 Å; N–H···O 160.3°], H–N(8b) and C(4b)═O(4b) [N(8b)···O(4b) = 2.85 Å; N–H···O 162.2°], H–N(9b) and C(5b)═O(5b) [N(9b)···O(5b) = 2.91 Å; N–H···O 157.7°] were observed. The distance between H-N(7b) and C(3b)═O(3b) (3.40 Å) was too long for an intramolecular hydrogen bond. In the packing mode, six intermolecular hydrogen bonds between H–O_w(d) and C(6b)═O(6b) [O_w(d)···O(6b) = 3.06 Å; O–H···O 172.1°], the H–O_w(e) and O_w(d) [O_w(e)···O_w(d) = 2.64 Å; O–H···O 175.6°], the H–O_w(e) and O_{MeOH} of the methanol [O_w(e)···O_{MeOH} = 2.87 Å; O–H···O 175.4°], the H–O_{MeOH} and O_{M9} of the methoxy group of (*R*,*R*)-Ac_5c^{dOM} [O_{MeOH}···O_{M9} = 2.77 Å; O–H···O 173.6°], the H–N(1b) and C(7b′)═O(7b′) [N(1b)···O(7b′) = 2.82 Å; N–H···O 164.4°] of a symmetry-related molecule (x, y, 1+z), and N(2b) and O_w(d′) [N(2b)···O_w(d′) = 2.89 Å; N–H···O 162.7°] of a symmetry-related molecule (x, y, 1+z) were observed. The α-helical chains of **A** and **B** were packed forming a head-to-tail alignment of chains ···**A**···**A**···**A**···**A**··· and ···**B**···**B**···**B**···**B**··· (Fig. 14).

The dominant conformations of four hexapeptides Cbz-(L-Leu-L-Leu-dAA)$_2$-OMe [dAA = **1**: Aib; **2**: Ac_5c; **3**: (*S*,*S*)-Ac_5c^{dOM}; **4**: (*R*,*R*)-Ac_5c^{dOM}] and four nonapeptides Boc-(L-Leu-L-Leu-dAA)$_3$-OMe [dAA = **5**: Aib; **6**: Ac_5c; **7**: (*S*,*S*)-Ac_5c^{dOM}; **8**: (*R*,*R*)-Ac_5c^{dOM}] in solution were found to be helical structures. Judging from the *R* value of the CD spectra in TFE/H_2O solution and in the solid state, Aib hexapeptide **1** and Ac_5c hexapeptide **2** formed right-handed (*P*) 3_{10}-helices, while Ac_5c^{dOM} hexapeptides **3** and **4** formed a mixture of (*P*) 3_{10}- and α-helices in solution and (*P*) α-helices in the solid state. The CD spectra of Aib nonapeptide **5** suggested the existence of a (*P*) 3_{10}-helix in solution and in the solid state, while those of Ac_5c nonapeptide **6** suggested the existence of a mixture of

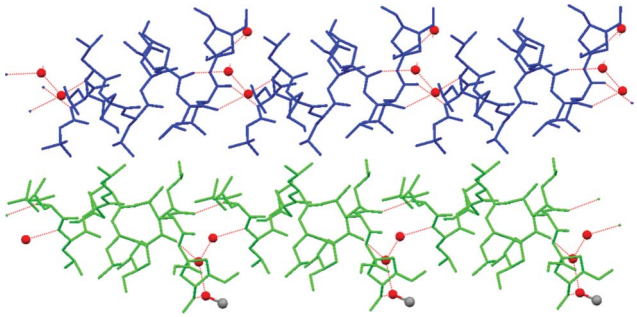

Fig. 14 Packing of **8** (molecule **A**: blue, molecule **B**: green) in the crystalline state. Intermolecular hydrogen bonds are indicated as red dashed lines.

(*P*) 3_{10}- and α-helices in solution and the existence of a 3_{10}-helix in the solid state. On the other hand, the CD spectra of chiral Ac_5c^{dOM} nonapeptides **7** and **8** indicated the existence of (*P*) α-helices in solution and in the solid state. X-ray crystallographic analysis revealed that the Aib hexapeptide **1** assumed a (*P*) 3_{10}-helix, while (*S*,*S*)-Ac_5c^{dOM} hexapeptide **3** assumed a (*P*) α-helix. Furthermore, the Ac_5c nonapeptide **6** and (*R*,*R*)-Ac_5c^{dOM} nonapeptide **8** were folded into (*P*) α-helices in the crystal state, and there was not much difference with the packing of the five-membered ring of the Ac_5c and Ac_5c^{dOM} residues (Fig. 15).

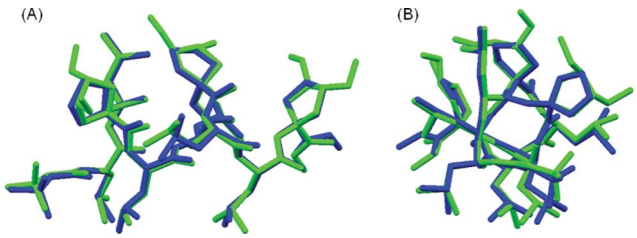

Fig. 15 The overlaid structures of nonapeptides **6** (molecule **A**: blue) and **8** (molecule **A**: green), as viewed (A) perpendicular to and (B) along to the helical axis.

Aib and Ac_5c are achiral amino acids, and thus do not have the bias for the helical-screw handedness. Therefore, the right-handed helical screw senses of L-Leu-based hexapeptides **1** and **2** and nonapeptides **5** and **6** were controlled by the chiral centers of L-Leu α-carbon atoms. On the other hand, (*S*,*S*)-Ac_5c^{dOM} and (*R*,*R*)-Ac_5c^{dOM} are chiral cyclic α,α-disubstituted α-amino acids, having chiral centers only at the side chain. The relationship between (*S*,*S*) and (*R*,*R*) is enantiomeric, thus the helical-screw properties of these cyclic amino acids should be opposite. All L-Leu hexapeptides and nonapeptides having chiral Ac_5c^{dOM} showed right-handed helical-screw sense. These results mean that L-Leu chiral centers on the α-carbon atoms are stronger than those of the side-chain chiral centers of Ac_5c^{dOM}. The Aib and achiral Ac_5c residues have the tendency to form (*P*) 3_{10}-helices in short L-Leu peptides, whereas the chiral Ac_5c^{dOM} residues have a penchant for forming (*P*) α-helices in short L-Leu peptides. The α-helical property of chiral Ac_5c^{dOM} may be due to the influence of the methoxy substituents, especially in terms of hydrophilicity and bulkiness on the cyclopentane ring. Therefore, the introduction of chiral Ac_5c^{dOM} residues at *i* and *i*+3 positions in the peptide may stabilize not a 3_{10}-helix but an α-helix by avoiding contact with the methoxy substituents of Ac_5c^{dOM} at *i* and *i*+3 positions.

Conclusions

In conclusion, four types of α,α-disubstituted amino acids: Aib, Ac_5c, (*S*,*S*)-Ac_5c^{dOM} and (*R*,*R*)-Ac_5c^{dOM}, were introduced into the L-leucine-based peptides and their influence on peptide conformation was studied. We demonstrated that the well-known achiral α,α-disubstituted amino acid Aib induces the 3_{10}-helical structure in short peptides, but the newly designed chiral cyclic α,α-disubstituted amino acids Ac_5c^{dOM} preferentially induce the α-helical structure. Although it has been believed that at least seven amino acid residues are necessary to construct α-helical peptides in the crystal state,[3,35–38] the L-Leu-hexapeptides containing chiral Ac_5c^{dOM} formed α-helices.[24,39] These results provide valuable information for the design of stable helical peptides and may also be applicable in many fields such as organic, bioorganic and medicinal chemistries.

Experimental

General remarks

FT-IR spectra were recorded on a Nicolet Avatar-320 spectrometer at 1 cm^{-1} resolution, with an average of 128 scans used for the solution ($CDCl_3$) method and a 0.1 mm path length for NaCl cells, or used for the attenuated total reflection (ATR) method.

CD spectra were recorded with a *Jasco J-720W* spectropolarimeter using a 1.0 mm path length cell. The data are expressed in terms of $[\theta]_M$, the total molar ellipticity (deg cm^2 $dmol^{-1}$). A mixture of 2,2,2-trifluoroethanol (TFE) and H_2O (50/50) was used as a solvent in solution, and a KCl disk was used in the solid state.

Single crystals of peptides **1**, **3** and **8** were grown from $MeOH/H_2O$, and that of **6** was from $EtOH/H_2O$. Data collection was performed on a Bruker AXS SMART 1000 CCD imaging plate diffractometer using graphite-monochromated Mo-Kα radiation. All crystals remained stable during the X-ray-data collection. The structures of the crystals were solved using the SHELXS 97[40] direct method and expanded by the Fourier technique.[41] All non-H-atoms were given anisotropic thermal parameters, some H-atoms were refined isotropically, and the remaining H-atoms at the calculated positions were given isotropic thermal parameters. The final cycle of full-matrix least-squares refinement of **1** gave an R_1 factor of 0.0434 based on 3417 ($I > 2\sigma(I)$) reflections and an *Rw* factor of 0.0870 for all data. The R_1 factor of **3** was 0.0522 based on 12192 ($I > 2\sigma(I)$) reflections and an *Rw* factor of 0.1427 for all data. The R_1 factor of **6** was 0.0962 based on 21523 ($I > 2\sigma(I)$) reflections and an *Rw* factor of 0.2635 for all data. The R_1 factor of **8** was 0.0859 based on 15919 ($I > 2\sigma(I)$) reflections and an *Rw* factor of 0.2370 for all data. All data for peptides **1**, **3**, **6** and **8** have been deposited in the Cambridge Crystallographic Data Centre (CCDC).†

Cbz-(L-Leu-L-Leu-Aib)$_2$-OMe (1)

Colorless crystals; mp 195–197 °C (recryst. from MeOH); $[\alpha]_D^{25}$ −11.4 (*c* 1.3, $CHCl_3$); IR (ATR solid state) 3314, 2956, 1745, 1654, 1527 cm^{-1}; ^1H NMR (400 MHz, $CDCl_3$) δ 7.55 (d, J = 7.8 Hz, 1H), 7.31–7.40 (m, 5H), 7.23–7.24 (br s, 2H), 7.19 (br s, 1H), 7.01 (br s, 1H), 6.32 (br s, 1H), 5.15 (dd, J = 12.4, 39.0 Hz, 2H), 4.33 (m, 1H), 4.17 (m, 1H), 3.87–3.98 (m, 2H), 3.65 (s, 3H), 1.40–1.87 (m, 24H), 0.73–0.97 (m, 24H); FAB(+)-MS *m/z* 811.4 (M^++Na); elemental analysis calcd for $C_{41}H_{68}O_9N_6$: C 62.41, H 8.69, N 10.65: found C 62.49, H 8.57, N 10.78.

Cbz-(L-Leu-L-Leu-Ac$_5$c)$_2$-OMe (2)

Colorless crystals; mp 98–100 °C (recryst. from $CHCl_3$); $[\alpha]_D^{25}$ −1.5 (*c* 1.0, $CHCl_3$); IR (ATR solid state) 3322, 2957, 1744, 1652, 1525 cm^{-1}; ^1H NMR (400 MHz, $CDCl_3$) δ 7.56 (d, J = 9.2 Hz, 1H), 7.42 (br s, 1H), 7.34–7.37 (m, 5H), 7.25 (br s, 1H), 7.17 (br s, 1H), 6.79 (br s, 1H), 5.68 (br s, 1H), 5.15 (dd, J = 12.4, 28.4 Hz, 2H), 4.10–4.16 (m, 2H), 3.88–3.95 (m, 2H), 3.69 (s,3H), 2.56 (m, 1H), 2.00–2.25 (m, 5H), 1.50–1.90 (m, 22H), 0.87–0.98 (m, 24H); FAB(+)-MS *m/z* 863.5 (M^++Na).

Cbz-[L-Leu-L-Leu-(*S*,*S*)-Ac$_5$c^{dOM}]$_2$-OMe (3)

Colorless crystals; mp 115–117 °C (recryst. from MeOH); $[\alpha]_D^{24}$ = +0.7 (*c* = 0.6, $CHCl_3$); IR (ATR solid state) 3335, 2956, 1742, 1654, 1531 cm^{-1}; ^1H NMR (400 MHz, $CDCl_3$) δ 7.54 (br s, 1H), 7.32–7.45 (m, 8H), 7.15 (br s, 1H), 6.24 (br s, 1H), 5.18 (dd, J = 12.4, 34.1 Hz, 2H), 4.32 (m, 1H), 4.21 (m, 1H), 3.67–4.01 (m, 6H), 3.64 (s, 3H), 3.31–3.35 (m, 12H), 2.94 (dd, J = 7.3, 14.0 Hz, 1H), 2.55–2.96 (m, 2H), 2.39–2.44 (m, 2H), 2.28 (dd, J = 7.3, 14.2 Hz, 1H), 2.07–2.17 (m, 2H), 1.97 (dd, J = 7.3, 13.9 Hz, 1H), 1.50–1.87 (m, 11H), 0.77–1.08 (m, 24H); FAB(+)-MS *m/z* 983.6 (M^++Na); elemental analysis calcd for $C_{49}H_{80}O_{13}N_6$: C 61.23, H 8.39, N 8.74: found C 61.24, H 8.35, N 8.98.

Cbz-[L-Leu-L-Leu-(*R*,*R*)-Ac$_5$c^{dOM}]$_2$-OMe (4)

Colorless crystals; mp 118–120 °C (recryst. from MeOH); $[\alpha]_D^{22}$ −22.9 (*c* 0.8, $CHCl_3$); IR (ATR solid state) 3321, 2957, 1743, 1652, 1534 cm^{-1}; ^1H NMR (400 MHz, $CDCl_3$) δ 7.52 (br s, 1H), 7.43 (br s, 1H), 7.34–7.39 (m, 7H), 7.00 (br s, 1H), 6.30 (br s, 1H), 5.20 (s, 2H), 4.34 (m, 1H), 4.22 (m, 1H), 3.73–3.95 (m, 6H), 3.62 (s, 3H), 3.29–3.33 (m, 12H), 3.05 (dd, J = 7.5, 14.4 Hz, 1H), 2.83 (dd, J = 7.1, 13.9 Hz, 1H), 2.58–2.66 (m, 2H), 2.28 (d, J = 19.3 Hz, 1H), 2.24 (dd, J = 7.1, 14.2 Hz, 1H), 1.49–2.02 (m, 14H), 0.83–0.99 (m, 24H): FAB(+)-MS *m/z* 983.6 (M^++Na); elemental analysis calcd for $C_{49}H_{80}O_{13}N_6$: C 61.23, H 8.39, N 8.74: found C 61.58, H 8.43, N 8.79.

Boc-(L-Leu-L-Leu-Aib)$_3$-OMe (5)

Colorless crystals; mp 191–193 °C (recryst. from MeOH); $[\alpha]_D^{24}$ −15.1 (*c* 1.0, $CHCl_3$); IR (ATR solid state) 3315, 2961, 1734, 1658, 1531 cm^{-1}; ^1H NMR (400 MHz, $CDCl_3$) δ 7.26–7.48 (m, 7H), 6.83 (d, J = 4.1 Hz, 1H), 5.31 (d, J = 2.8 Hz, 1H), 4.32 (m, 1H), 4.14 (m, 1H), 3.85–4.04 (m, 4H), 3.66 (s, 3H), 1.40–1.79 (m, 45H), 0.84–1.09 (m, 36H); FAB(+)-MS *m/z* 1088.7 (M^++Na); elemental analysis calcd for $C_{54}H_{99}O_{12}N_9$: C 60.82, H 9.36, N 11.82: found C 60.73, H 9.34, N 11.91.

Boc-(L-Leu-L-Leu-Ac$_5$c)$_3$-OMe (6)

Colorless crystals; mp 213–215 °C (recryst. from $CHCl_3$); $[\alpha]_D^{24}$ = +6.8 (*c* = 1.0, $CHCl_3$); IR (ATR solid state) 3313, 2957, 1740, 1652, 1529 cm^{-1}; ^1H NMR (400 MHz, $CDCl_3$) δ 7.66 (d, J = 4.6 Hz, 1H), 7.57 (br s, 1H), 7.45–7.48 (m, 3H), 7.35 (d, J = 5.9 Hz, 1H), 7.24 (br s, 1H), 6.55 (br s, 1H), 5.06 (br s, 1H), 4.34 (m, 1H), 4.19 (m, 1H), 3.88–4.02 (m, 4H), 3.66 (s, 3H), 2.60–2.65 (m, 2H),

2.07–2.24 (m, 6H), 1.58–1.94 (m, 34H), 1.56 (s, 9H), 0.79–1.00 (m, 36H): FAB(+)-MS *m/z* 1144 (M^++H); elemental analysis calcd for $C_{60}H_{105}O_{12}N_9$: C 62.96, H 9.25, N 11.01: found C 62.94, H 9.24, N 10.86.

Boc-[L-Leu-L-Leu-(*S*,*S*)-Ac_5c^{dOM}]$_3$-OMe (7)

Colorless crystals; mp 110–112 °C (recryst. from MeOH); $[\alpha]_D^{24}$ = +19.6 (*c* = 1.35, $CHCl_3$); IR (ATR solid state); 3321, 2960, 1736, 1661, 1529 cm^{-1}; ^1H NMR (400 MHz, $CDCl_3$) δ 7.68 (d, *J* = 4.6 Hz, 1H), 7.34–7.46 (m, 6H), 6.94 (d, *J* = 2.6 Hz, 1H), 5.22 (d, *J* = 3.7 Hz, 1H), 4.28 (m, 1H), 4.18 (m, 1H), 3.89–4.05 (m, 5H), 3.67–3.83 (m, 5H), 3.66 (s, 3H), 3.30–3.36 (m, 18H), 2.97 (dd, *J* = 7.3, 13.8 Hz, 1H), 2.63–2.77 (m, 3H), 2.18–2.37 (m, 5H), 2.08 (dd, *J* = 7.6, 14.2 Hz, 1H), 1.52–2.03 (m, 20H), 1.49 (s, 9H), 0.88–1.10 (m, 36H); FAB(+)-MS *m/z* 1346.9 (M^++Na); elemental analysis calcd for $C_{66}H_{117}O_{18}N_9$: C 59.84, H 8.90, N 9.52: found C 60.17, H 8.91, N 9.65.

Boc-[L-Leu-L-Leu-(*R*,*R*)-Ac_5c^{dOM}]$_3$-OMe (8)

Colorless crystals; mp 170–172 °C (recryst. from MeOH); $[\alpha]_D^{24}$ −6.65 (*c* 0.85, $CHCl_3$); IR (ATR solid state) 3330, 2960, 1736, 1658, 1532 cm^{-1}; ^1H NMR (400 MHz, $CDCl_3$) δ 7.75 (d, *J* = 5.1 Hz, 1H), 7.70 (br s, 1H), 7.58 (d, *J* = 5.3 Hz, 1H), 7.55 (br s, 1H), 7.51 (br s, 1H), 7.40 (d, *J* = 5.05 Hz, 1H), 7.38 (br s, 1H), 6.72 (br s, 1H), 5.43 (br s, 1H), 4.36 (m, 1H), 4.20 (m, 1H), 3.76–4.00 (m, 10H), 3.69 (s, 3H), 3.25–3.38 (m, 18H), 3.19 (dd, *J* = 7.6, 14.3 Hz, 1H), 3.01 (dd, *J* = 6.2, 14.4 Hz, 1H), 2.70–2.94 (m, 2H), 2.64–2.68 (m, 2H), 2.14–2.24 (m, 2H), 1.61–2.00 (m, 22H), 1.54 (s, 9H), 0.85–1.02 (m, 36H); FAB(+)-MS *m/z* 1346.9 (M^++Na); elemental analysis calcd for $C_{66}H_{117}O_{18}N_9$: C 59.84, H 8.90, N 9.52: found C 60.15, H 8.91, N 9.62.

Acknowledgements

This work was supported in part by a Grant-in-Aid for Young Scientists (B) (21790018) from the Ministry of Education, Science, Sports and Culture of Japan, and a Grant-in-Aid for Scientific Research (B) (22390022) from Japan Society for the Promotion of Science.

Notes and references

1 J. P. Schneider and J. W. Kelly, *Chem. Rev.*, 1995, **95**, 2169–2187.
2 J. Venkatraman, S. C. Shankaramma and P. Balaram, *Chem. Rev.*, 2001, **101**, 3131–3152.
3 C. Toniolo, M. Crisma, F. Formaggio, C. Peggion, Q. B. Broxterman and B. Kaptein, *J. Inclusion Phenom. Macrocyclic Chem.*, 2005, **51**, 121–136.
4 S. H. Gellman, *Acc. Chem. Res.*, 1998, **31**, 173–180.
5 H. Heimgartner, *Angew. Chem., Int. Ed. Engl.*, 1991, **30**, 238–264.
6 E. Benedetti, V. Barone, A. Bavoso, D. B. Blasio, F. Lelj, V. Pavone, C. Pedone, G. M. Bonora, C. Toniolo, M. T. Leplawy, K. Kaczmarek and A. Redlinski, *Biopolymers*, 1988, **27**, 357–371.
7 C. Toniolo, G. M. Bonora, A. Bavoso, E. Benedetti, B. Di Blasio, V. Pavone, C. Pedone, V. Barone, F. Lelj, M. T. Leplawy, K. Kaczmarek and A. Redlinski, *Biopolymers*, 1988, **27**, 373–379.
8 C. Toniolo, M. Crisma, F. Formaggio, C. Valle, G. Cavicchioni, G. Precigoux, A. Aubry and J. Kamphuis, *Biopolymers*, 1993, **33**, 1061–1072.
9 F. Formaggio, A. Barazza, A. Bertocco, C. Toniolo, Q. B. Broxterman, B. Kaptein, E. Brasola, P. Pengo, L. Pasquato and P. Scrimin, *J. Org. Chem.*, 2004, **69**, 3849–3856.
10 M. Crisma, M. Saviano, A. Moretto, Q. B. Broxterman, B. Kaptein and C. Toniolo, *J. Am. Chem. Soc.*, 2007, **82**, 15471–15473.
11 B. Jaun, M. Tanaka, P. Seiler, F. N. M. Kühnle, C. Braun and D. Seebach, *Liebigs Ann./Recl.*, 1997, 1697–1710.
12 M. Tanaka, *Chem. Pharm. Bull.*, 2007, **55**, 349–358.
13 I. L. Karle and P. Balaram, *Biochemistry*, 1990, **29**, 6747–6756.
14 M. Crisma, E. Andreetto, M. D. Zotti, A. Moretto, C. Peggion, F. Formaggio and C. Toniolo, *J. Pept. Sci.*, 2007, **13**, 190–205.
15 S. Aravinda, N. Shamala and P. Balaram, *Chem. Biodiversity*, 2008, **5**, 1238–1262.
16 A. Moretto, I. Menegazzo, M. Crisma, E. J. Shotton, H. Nowell, S. Mammi and C. Toniolo, *Angew. Chem., Int. Ed.*, 2009, **48**, 8986–8989.
17 M. Oba, Y. Demizu, N. Yamagata, Y. Sato, M. Doi, M. Tanaka, H. Suemune, H. Okuda and M. Kurihara, *Tetrahedron*, 2010, **66**, 2293–2296.
18 Y. Demizu, N. Yamagata, Y. Sato, M. Doi, M. Tanaka, H. Okuda and M. Kurihara, *J. Pept. Sci.*, 2010, **16**, 153–158.
19 Y. Demizu, M. Doi, Y. Sato, M. Tanaka, H. Okuda and M. Kurihara, *J. Org. Chem.*, 2010, **75**, 5234–5239.
20 M. Tanaka, Y. Demizu, M. Doi, M. Kurihara and H. Suemune, *Angew. Chem., Int. Ed.*, 2004, **43**, 5360–5363.
21 Y. Demizu, M. Tanaka, M. Doi, M. Kurihara, H. Okuda and H. Suemune, *J. Pept. Sci.*, 2010, **16**, 621–626.
22 S. Royo, W. M. De Borggraeve, C. Peggion, F. Formaggio, M. Crisma, A. I. Jiménez, C. Cativiela and C. Toniolo, *J. Am. Chem. Soc.*, 2005, **127**, 2036–2037.
23 M. Tanaka, K. Anan, Y. Demizu, M. Kurihara, M. Doi and H. Suemune, *J. Am. Chem. Soc.*, 2005, **127**, 11570–11571.
24 Preliminary communication of this paper was published. See: Y. Demizu, M. Tanaka, M. Nagano, M. Kurihara, M. Doi, T. Maruyama and H. Suemune, *Chem. Pharm. Bull.*, 2007, **55**, 840–842.
25 M. Nagano, M. Doi, M. Kurihara, H. Suemune and M. Tanaka, *Org. Lett.*, 2010, **12**, 3564–3566.
26 J. Sheehan, P. Cruickshank and G. Boshart, *J. Org. Chem.*, 1961, **26**, 2525–2528.
27 J. Sheehan and G. P. Hess, *J. Am. Chem. Soc.*, 1955, **77**, 1067–1068.
28 D. F. Kennedy, M. Crisma, C. Toniolo and D. Chapman, *Biochemistry*, 1991, **30**, 6541–6548.
29 M. Tanaka, S. Nishimura, M. Oba, Y. Demizu, M. Kurihara and H. Suemune, *Chem.–Eur. J.*, 2003, **9**, 3082–3090.
30 C. Toniolo, G. M. Bonora, A. Bavoso, E. Benedetti, B. Di Blasio, V. Pavone, C. Pedone, V. Barone, F. Lelj, M. T. Leplawy, K. Kaczmarek and A. Redlinski, *Biopolymers*, 1988, **27**, 373–379.
31 C. Toniolo, A. Polese, F. Formaggio, M. Crisma and J. Kamphuis, *J. Am. Chem. Soc.*, 1996, **118**, 2744–2745.
32 F. Formaggio, M. Crisma, P. Rossi, P. Scrimin, B. Kaptein, Q. B. Broxterman, J. Kamphuis and C. Toniolo, *Chem.–Eur. J.*, 2000, **6**, 4498–4504.
33 L. Pal, G. Basu and P. Chakrabarti, *Proteins: Struct., Funct., Genet.*, 2002, **48**, 571–579.
34 R. Bardi, A. M. Pizzesi, C. Toniolo, M. Sukumar and P. Balaram, *Biopolymers*, 1986, **25**, 1635–1644.
35 C. Toniolo, M. Crisma, F. Formaggio, C. Peggion, Q. B. Broxterman and B. Kaptein, *Biopolymers*, 2004, **76**, 162–176.
36 M. Crisma, F. Formaggio, A. Moretto and C. Toniolo, *Biopolymers*, 2006, **84**, 3–12.
37 V. Pavone, E. Benedetti, B. Di Blasio, C. Pedone, A. Santini, A. Bavoso, C. Toniolo, M. Crisma and L. Satore, *J. Biomol. Struct. Dyn.*, 1990, **7**, 1321–1331 .
38 M. Crisma, M. Saviano, A. Moretto, Q. B. Broxterman, B. Kaptein and C. Toniolo, *J. Am. Chem. Soc.*, 2007, **129**, 15471–15473.
39 Six residues are enough to construct an α-helical peptide in solution: A. Moretto, F. Formaggio, B. Kaptein, Q. B. Broxterman, L. Wu, T. A. Keiderling and C. Toniolo, *Biopolymers*, 2008, **90**, 567–574.
40 G. M. Sheldrick, *SHELXL 97. Program for Crystal Structure Refinement.* University of Göttingen: Göttingen (1997).
41 P. T. Beurskens, G. Admiraal, G. Beurskens, W. P. Bosman, R. de Gelder, R. Israel, J. M. M. Smits, *The DIRDIF-99 program system, Technical Report of the Crystallography Laboratory*, University of Nijmegen, The Netherlands (1994).

